

A Dynamic Simulation Model for Semiconductor Laser Diodes

Toby Schaer, Robert Rusnov, Stephen Eagle, Jay Jastrebski, Steven Albanese and Xavier Fernando

Abstract - A method for using the popular math packages MATLAB and Simulink to simulate the behaviour of distributed feedback quantum-well semiconductor laser diodes using the rate equations that describe them is presented. A large-signal model for threshold determination and operating point selection is discussed. Small-signal properties of interest can be investigated using a state-space description of a linearized version of the rate equations, based on their Jacobian.

The techniques presented here are suitable for investigation of both analog and digital modulation performance, for example frequency and pulse response. Large signal gain-saturation and frequency modulation effects are not considered.

I. INTRODUCTION

Modern high-speed data transmission is accomplished with fiber optic systems, which generally consist of a laser light source, the fiber itself, and a detector. The most common light source is the semiconductor laser diode because of its small size, ruggedness, and manufacturing cost compared to other laser emitters.

A cost-effective method of data transmission is direct modulation of the laser diode drive current combined with a photodetector at the other end. This scheme is known as Intensity Modulation/Direct Detection, or IM/DD. One of the factors limiting the data rate is the switching speed of the laser diode. Improving the characteristics of the diode is thus an area of extreme interest.

II. A BRIEF REVIEW OF THE RATE EQUATIONS

The behaviour of a semiconductor laser diode is modeled with a set of three differential equations which describe the mechanism by which an electrical current causes stimulated photon emission. There are many forms of these equations, but in this paper we use a modified form of Tucker's equations [1] employed by Bjerkan et al. [3]:

$$\frac{dN(t)}{dt} = \frac{I(t)}{q \cdot V_a} - g_o \frac{[N(t) - N_o] \cdot S(t)}{1 + \epsilon \cdot S(t)} - \frac{N(t)}{\tau_n} \quad (1)$$

$$\frac{dS(t)}{dt} = \Gamma \cdot g_o \frac{[N(t) - N_o] \cdot S(t)}{1 + \epsilon \cdot S(t)} - \frac{S(t)}{\tau_p} + \frac{\Gamma \cdot \beta}{\tau_n} \cdot N(t) \quad (2)$$

$$\frac{d\phi(t)}{dt} = \frac{1}{2} \alpha \left[\Gamma \cdot g_o [N(t) - N_o] - \frac{1}{\tau_p} \right] \quad (3)$$

Equation (1) is the rate equation for carrier density, photon density is given by Equation (2), and optical phase by Equation (3). This is a large-signal model that describes laser diode behaviour in both the spontaneous emission and stimulated emission region. The nonlinear saturation region (see Figure 2) due to junction heating is not included in this model. Additionally, the optical power generated (also described in [3]) by the diode is:

$$p(t) = \frac{S(t)V_a\eta_o h\nu}{2\Gamma\tau_p} \quad (4)$$

Coefficients are defined in Appendix A.

III. THEORY

The large signal single-mode rate equations as given in Eq.1 and Eq.2 were used to build the initial model. This model's purpose was to identify the various regions of operation of the laser diode based on the parameters found in the article by Javro and Kang [2]. Building the large signal model was essential in determining operating points within the 'semi' linear lasing region. It is these operating points, once the lasing region was defined above threshold, that were used to characterize the small signal response. As depicted in Figure 2, this is in the linear stimulated emission region.

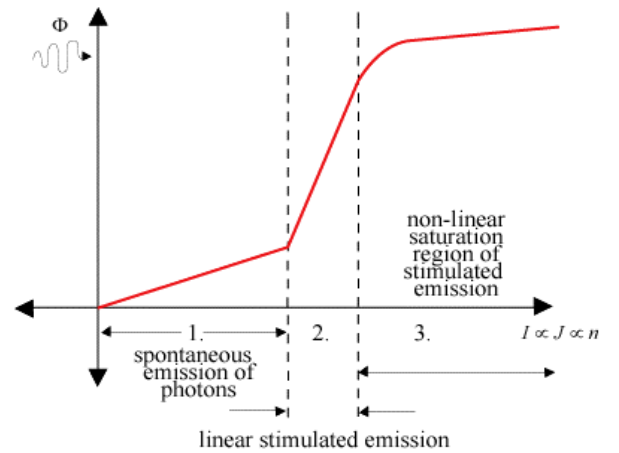


Figure 2. Full operating region of laser diode (large-signal).

The problem with finding a closed form solution to the rate equations lies in the fact that the equations are cross-coupled by the product term containing both the pho-

ton and electron density. For example, the standard Laplace Transform approach would fail because it is suitable only for linear, constant coefficient differential equations. Setting each equation to zero and solving the resulting system merely linearizes the rate equations about the threshold (N_{th}). Simply, this leaves the state-space matrix with linearly inseparable terms. The solution to this was to linearize the equations by creating a Jacobian matrix. This new matrix contains constant coefficient terms when evaluated at specific operating points. The ultimate goal was to linearize the rate equations and use them in a state-space model for small signal simulation.

In order to obtain values to simulate the small signal response, the non-linear rate equations were linearized by taking the partial derivative of each time-dependent term with respect to photon and electron density. It is this new model that allows the results of the large signal response to be used in simulating the small signal response.

The process was as follows: Choose an arbitrary operating point close to the threshold, such that the gain saturation term $1/(1 + \epsilon S(t))$ will approach 1 for values of $\epsilon S(t) \ll 1$. This term will have negligible effect on Eq.1 and Eq.2 and partial derivatives with respect to $N(t)$ and $S(t)$ can safely be taken.

$$\frac{\partial \left(\frac{dN(t)}{dt} \right)}{\partial N(t)} = -\frac{1}{\tau_n} - g_o \cdot S(t) \quad (7)$$

$$\frac{\partial \left(\frac{dN(t)}{dt} \right)}{\partial S(t)} = -g_o \cdot [N(t) - N_o] \quad (8)$$

$$\frac{\partial \left(\frac{dS(t)}{dt} \right)}{\partial N(t)} = \Gamma \cdot g_o \cdot S(t) + \frac{\Gamma \cdot \beta}{\tau_n} \quad (9)$$

$$\frac{\partial \left(\frac{dS(t)}{dt} \right)}{\partial S(t)} = \Gamma \cdot g_o \cdot [N(t) - N_o] - \frac{1}{\tau_p} \quad (10)$$

Now using the Jacobian matrix in a state-space model,

$$\begin{bmatrix} \dot{N} \\ \dot{S} \end{bmatrix} = \begin{bmatrix} \frac{\partial \left(\frac{dN}{dt} \right)}{\partial n} & \frac{\partial \left(\frac{dN}{d\Phi} \right)}{\partial \Phi} \\ \frac{\partial \left(\frac{dS}{dt} \right)}{\partial n} & \frac{\partial \left(\frac{dS}{d\Phi} \right)}{\partial \Phi} \end{bmatrix} \cdot \begin{bmatrix} N \\ S \end{bmatrix} + \begin{bmatrix} 1 \\ 0 \end{bmatrix} \cdot I(t) \quad (11)$$

$$y = [0 \quad 1] \cdot \begin{bmatrix} N \\ S \end{bmatrix}$$

The final result was the following state-space model,

$$\begin{bmatrix} \dot{N} \\ \dot{S} \end{bmatrix} = \begin{bmatrix} -\frac{1}{\tau_n} - g_o \cdot S_{op} & -g_o \cdot [N_{op} - N_o] \\ \Gamma \cdot g_o \cdot S_{op} + \frac{\Gamma \cdot \beta}{\tau_n} & \Gamma \cdot g_o \cdot [N_{op} - N_o] - \frac{1}{\tau_p} \end{bmatrix} \cdot \begin{bmatrix} N \\ S \end{bmatrix} + \begin{bmatrix} 1 \\ 0 \end{bmatrix} \cdot I(t) \quad (12)$$

$$y = [0 \quad 1] \cdot \begin{bmatrix} N \\ S \end{bmatrix}$$

where S_{op} and N_{op} indicate the respective steady-state photon and electron densities for an arbitrary bias current. Figure 3 illustrates the selection of a particular operating point within the lasing region of the diode.

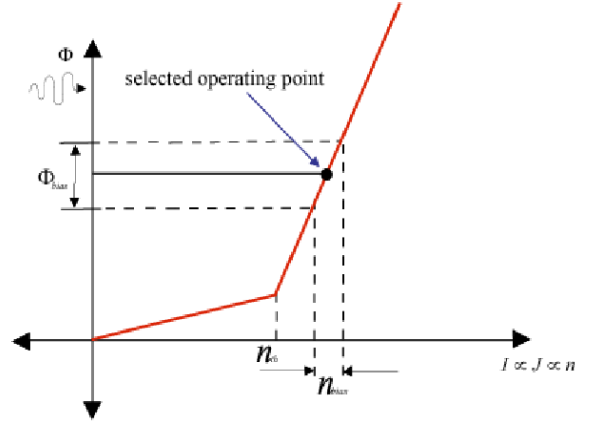


Figure 3. Example of operating point.

IV. LARGE SIGNAL SIMULATION MODEL

The full equation model given by Eqs. (1) and (2) was modeled in Simulink. The method used to transform the equations into a signal-flow diagram is borrowed from the field of analog computation – the equations were *mechanized* into a model that gives numerical solutions for arbitrary inputs and time scales that are of interest. The model is shown in Figure 4.

V. LASER OPERATING REGIONS

A ramp input was applied to the model to obtain a graph similar to Figure 2. The simulation was run over a time period that was several orders of magnitude longer than the turn-on transient effects that happen near threshold, to avoid the oscillatory behaviour in both $N(t)$ and $S(t)$ in this region. All simulations used a standard 4th-order Runge-Kutta algorithm with a fixed step size of 1ps as an equation solver. The model parameters are those used in [2], and are given for reference in Appendix A. A maximum of 20mA of pumping current was used, and simulations were run including the e terms, and without. The resulting $I(t)$ vs. $P(t)$ graphs are shown superimposed in Figure 5.

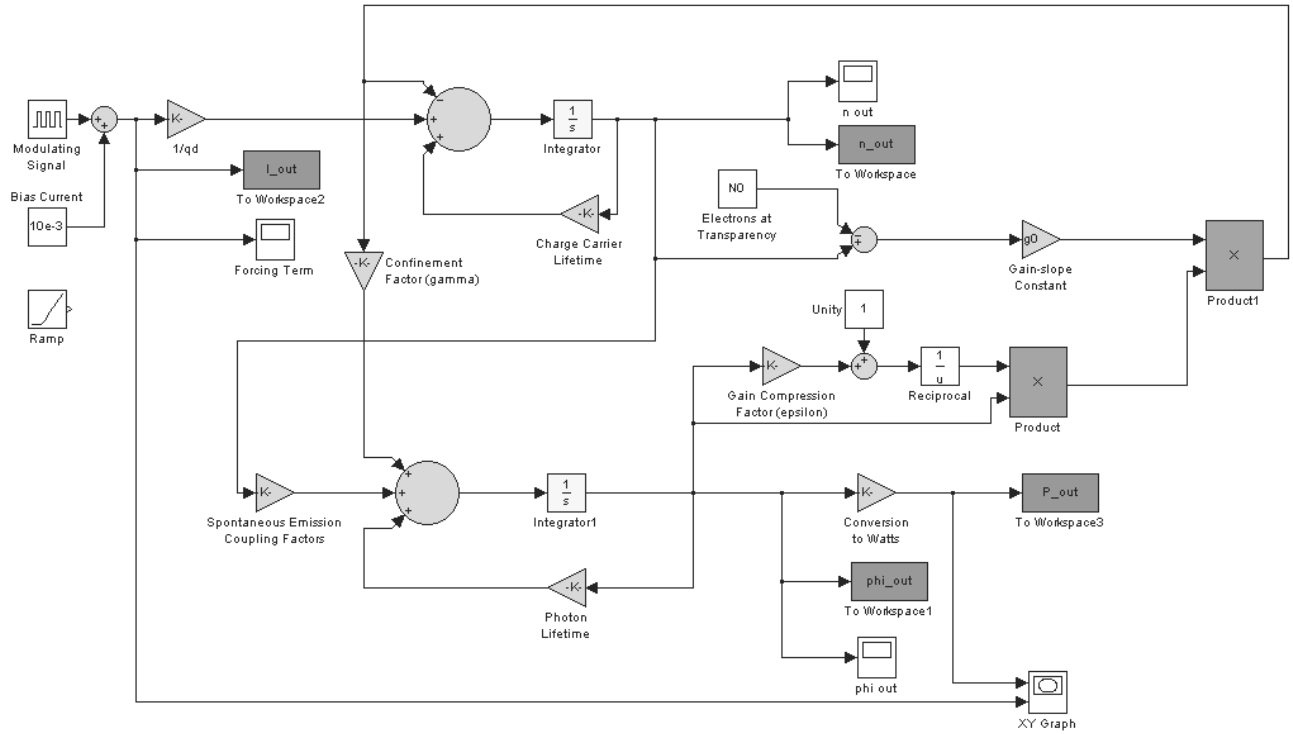


Figure 4: Large-Signal Simulink Model

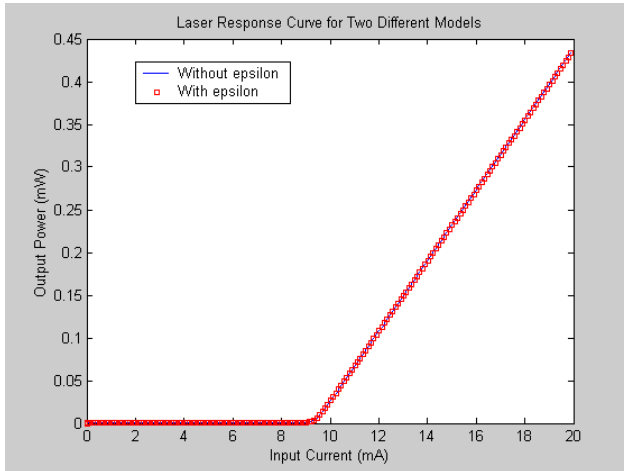


Figure 5: Laser Response Curves

It is worth noting that the previous assumption of neglecting the effect of ϵ (the gain saturation parameter) near threshold is valid.

From Figure 5 it is possible to determine the value of the threshold current graphically, by extrapolation, as shown in Figure 6. The threshold current $I_{th} = 9.32mA$. This sets a lower limit on the selection range of the operating points.

The Simulink model was again employed to find numerical solutions for the operating points, given a constant pumping current. Two bias points above threshold were computed:

Pumping Current (mA)	Electron Density (m^{-3})	Photon Density (m^{-3})
10mA	1.9531×10^{18}	1.9221×10^{13}
15mA	1.9571×10^{18}	1.7141×10^{14}

Table I. Operating Points.

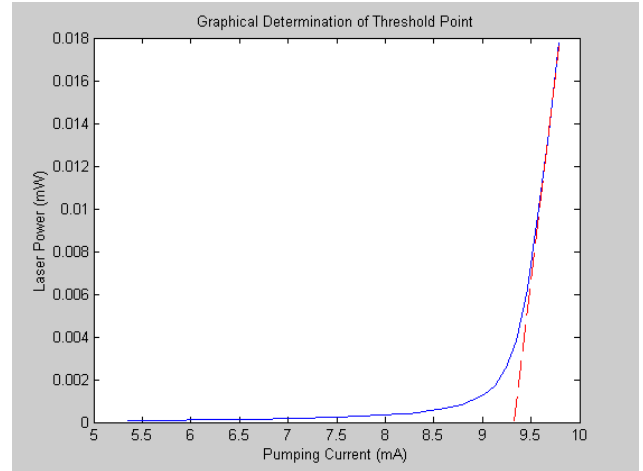


Figure 6: Laser Threshold Current

VI. SMALL SIGNAL SIMULATIONS

With the operating points from Table I, the Jacobian matrix of Eqs. (7) through (10) could be evaluated and a state-space model generated for each. A MATLAB script used for this purpose is shown in Appendix B.

This now permits an analysis of frequency response, for analog modulation purposes, and pulse response for digital modulation. Frequency modulation effects such as chirping were not simulated. Note that the output of the model is photon density, not optical power, which explains some of the large gains in the Bode plots!

VII. BODE PLOTS OF FREQUENCY RESPONSE

Both models were analyzed close to their corner frequen-

cies. From the state-space model it is clear that the laser diode is a second-order system with no zeros, a fact verified by the Bode phase plots. Figures 7 & 8 show the response of the 10mA system, while 9 & 10 show the 15mA system.

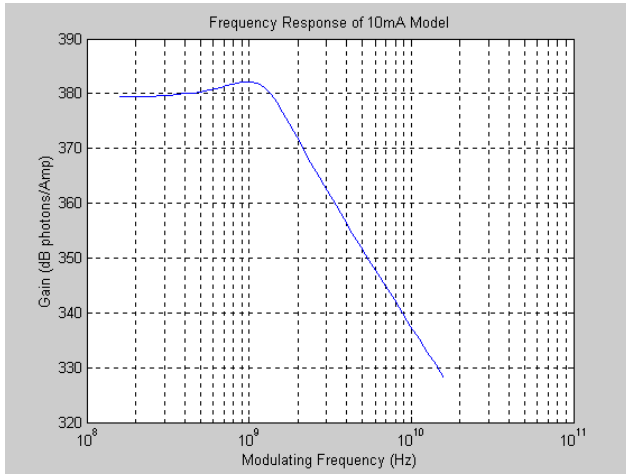


Figure 7: Magnitude Response of 10mA Model.

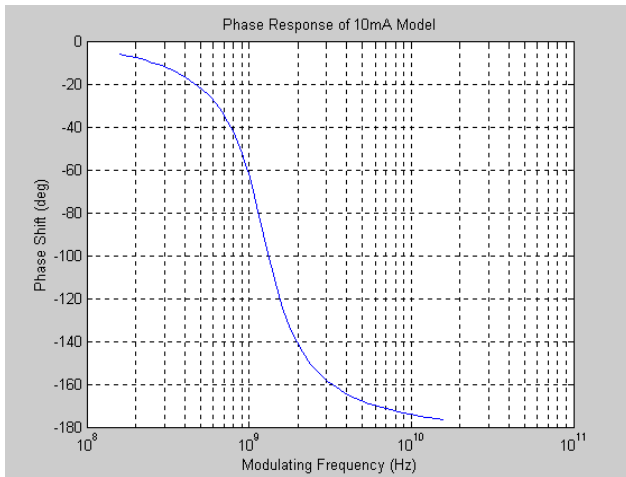


Figure 8: Phase Response of 10mA System

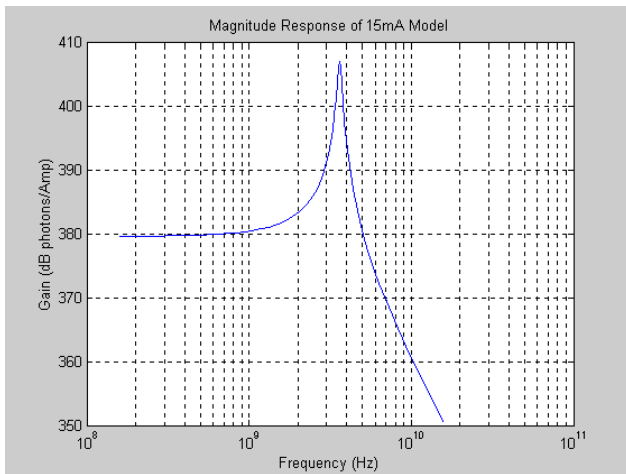


Figure 9: Magnitude Response of 15mA System

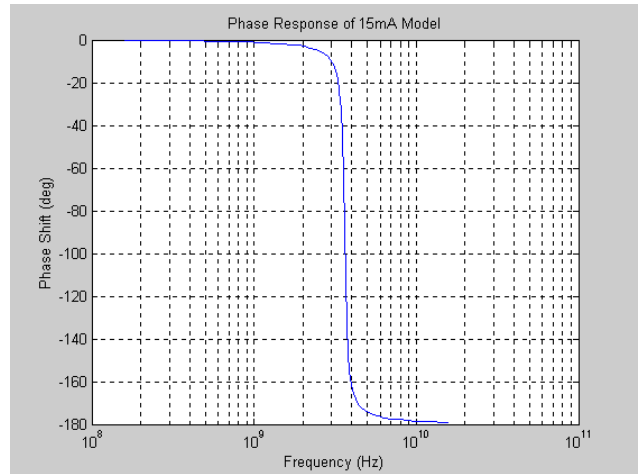


Figure 10: Phase Response of 15mA System

VIII. PULSE MODULATION

Both models were modulated with a 2ns pulse of 1mA above the operating point. Figures 11 and 12 show the 10mA and 15mA models, respectively. The response worsens with increased bias current, therefore only the 10mA model was tried with a 1ns pulse of 1mA (see Figure 13).

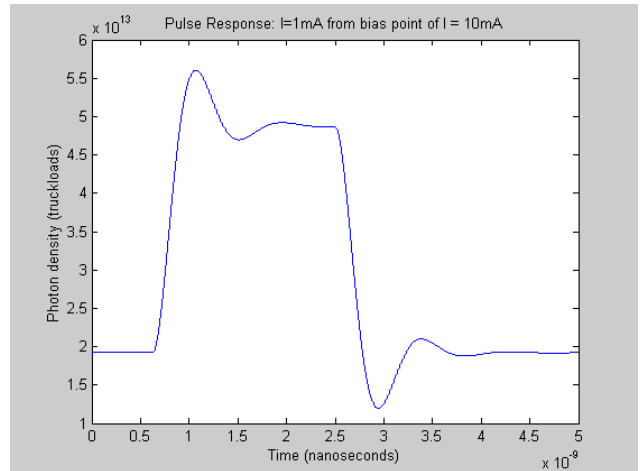


Figure 11: 10mA Model Response to 2ns, 1mA Pulse

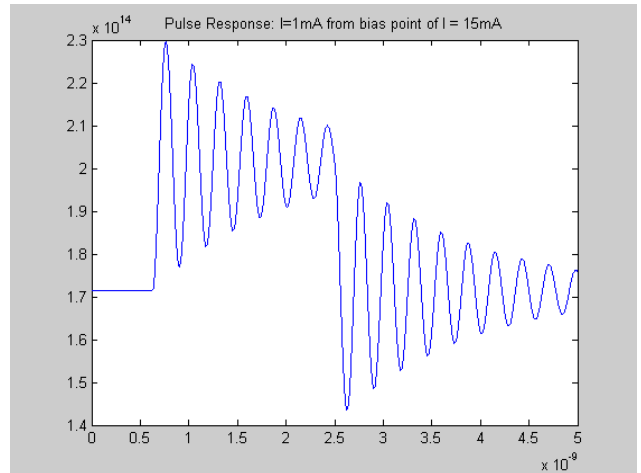


Figure 12: 15mA Model Response to 2ns, 1mA Pulse

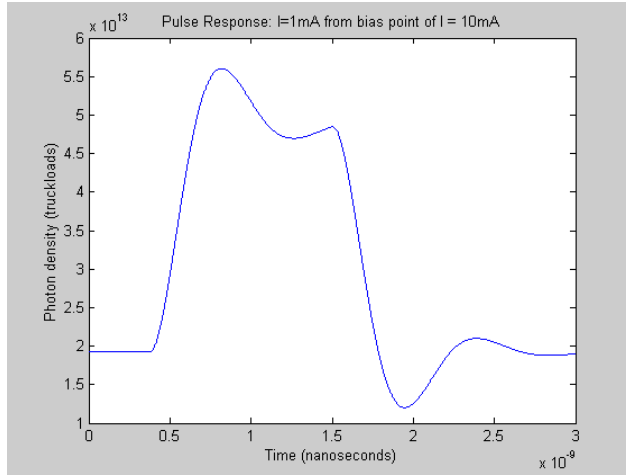


Figure 13: 10mA Model Response to 1ns, 1mA Pulse

IX. SUMMARY

This paper presented a method for simulating a quantum-well distributed feedback (QW-DFB) semiconductor laser diode based on the rate equations describing it. A large-signal model was constructed to find the threshold current of the diode, and to identify a relatively linear region above threshold for operating point selection. The large signal model also proved useful for finding numerical solutions for the steady-state values of electron and photon densities for currents above threshold.

The small-signal analysis was conducted using a linearized state-space description, based on taking the Jacobian of Eqs. (1) and (2), and evaluating at the operating points previously computed by the large-signal model. This model was shown to be an aid in determining the frequency response (and thus the bandwidth) of a laser diode for analog modulation purposes, and modeling the pulse response (and from this, the maximum bitrate) for digital modulation techniques.

Example results are given to illustrate the simulation approach and to verify its validity. The advantages of the approach presented here are its relative ease of automation, graphical model construction, and interactive control of simulation parameters. Detailed studies of specific devices can thus be carried out efficiently.

X. REFERENCES

- [1] R.S. Tucker & D.J. Pope, "Large Signal Circuit Model for Simulation of Injection-Laser Modulation Dynamics," *IEEE J. Quantum Electron.*, vol. QE-19, pp.1179-1183, July 1983.
- [2] S.A. Javro & S.M. Kang, "Transforming Tucker's Linearized Laser Rate Equations to a Form that has a Single Solution Regime," *Journal of Lightwave Technology*, vol.13, No.9, pp.1899-1904, September 1995.
- [3] L. Bjerkan, A. Royset, L. Hafskjaer, and D.Myhre, "Measurement of Laser Parameters for Simulation of High-Speed Fibre Optic Systems," *Journal of Lightwave Technology*, vol.14, No.5, pp.839-850, May 1996.
- [4] G. Keiser, *Optical Fiber Communications*. New York: McGraw-Hill, 2000, pp. 161-193.

APPENDIX A LIST OF SYMBOLS

Symbol	Value	Dimension	Description
$I(t)$	-	A	laser current
$S(t)$	-	m^{-3}	photon density
Γ	0.44	—	optical confinement factor
g_s	3.0×10^8	cm^{-3}/s	gain slope
$N(t)$	-	m^{-3}	carrier density
N_0	1.2×10^{18}	cm^{-3}	carrier density at transparency
ϵ	3.4×10^{17}	cm^{-3}	gain saturation parameter
τ_p	1.0×10^{12}	s	photon lifetime
β	4.0×10^{-4}	—	spontaneous emission factor
τ_n	3.0×10^7	s	carrier lifetime
V_a	9.0×10^{11}	cm^3	volume of the active region
Φ	-	—	phase of the electric field from the laser
α	-	—	line-width enhancement factor
$P(t)$	-	W	optical power from the laser
q	1.602×10^{19}	C	electronic charge
η	0.1	—	total quantum efficiency
h	6.624×10^{-34}	J-s	Plank's constant
$\Delta\nu$	-	s^{-1}	instantaneous optical frequency deviation
D	-	s/m^2	fibre dispersion coefficient
L	-	m	fibre length

APPENDIX B

% smallsig.m : Linearized state-space laser diode model. T.Schaer March 2002

clear all; close all; echo off

% Operating Point Values, obtained from Simulink Model

n_10 = 1.9531e18; s_10 = 1.9221e13;
n_15 = 1.9571e18; s_15 = 1.7141e14;

% Other constants (Javro & Kang)

q = 1.6e-19; Va = 9e-11;
tn = 3e-9; tp = 1e-12;
gamma = 0.44; beta = 4e-4;
N0 = 1.2e18; g0 = 3e-6;
eta = 0.1; h = 6.624e-34;
f = 1.997e14;

% Hand-derived Jacobian matrix

A_10 = [-g0*s_10-1/tn -g0*(n_10 - N0); gamma*g0*s_10+gamma*beta/tn gamma*g0*(n_10 - N0)-1/tp]
A_15 = [-g0*s_15-1/tn -g0*(n_15 - N0); gamma*g0*s_15+gamma*beta/tn gamma*g0*(n_15 - N0)-1/tp]

% Remaining Matrices

B = [(1/(q*Va)); 0]
C = [0 1]
D = 0

% Check controllability & observability of model

if(rank(ctrb(A_10,B))==2)
disp('System is controllable for this operating point');
end

if(rank(observ(A_10,C))==2)
disp('System is observable for this operating point');
end

% Generate time vector in a useful range (0-14ns)

t = 0:0.0001:14;
t = t*1e-9;

% Matching step input: step time at 1/8 of sim run length, amplitude = 1mA

t_step = round(length(t)/8);
u = [zeros(1,t_step+1) ones(1,(3*t_step))] zeros(1,4*t_step);
u = u*1e-3;

% Generate state-space objects

sys = ss(A_10,B,C,D); sys_15 = ss(A_15,B,C,D);

% Simulate response to input

y = lsim(sys,u,t); y2 = lsim(sys_15,u,t);

% recall that laser is already on: add steady-state values

y = s_10*ones(length(y),1) + y; y2 = s_15*ones(length(y2),1) + y2;

plot(t,y)
xlabel('Time (nanoseconds)'); ylabel('Photon density (1/m^3)');
title('Pulse Response: I=1mA from bias point of I = 10mA');

figure
plot(t,y2)
xlabel('Time (nanoseconds)');
title('Pulse Response: I=1mA from bias point of I = 15mA');